CFSRC COLLOQUIUM

Proceedings of the Cold-Formed Steel Research Consortium Colloquium
17-19 October 2022 (cfsrc.org)

Non-linear performance of topology optimized orthotropic bare steel deck diaphragms

Astrid Winther Fischer[1], Federico Ferrari[2], James K. Guest[3], Benjamin W. Schafer[4]

Abstract

The objective of this paper is to compare the elasto-plastic response of traditional and optimized roof diaphragm designs under lateral loads. The seismic building design depends on the floor and roof diaphragms can transfer lateral loads to the vertical lateral force resisting systems and ensure continued global stability of the structure during seismic events. Diaphragms have traditionally been designed to remain elastic, but researchers have observed that diaphragms experience inelastic deformations in earthquakes. Work in a recent paper used topology optimization to design bare steel deck diaphragms by optimizing the deck selection and deck orientations assuming linear elastic behavior. The optimized designs as well as traditional designed diaphragms are subjected to a non-linear pushover analysis assuming the deck plasticization is solely governed by shear deformations and reduction in shear stiffness. It was found that the optimized designs outperform typical deck designs in terms of ultimate bearing capacity and energy dissipation despite being optimized with respect to linear stiffness alone. It is hoped that these findings will encourage further research into the design of diaphragm decks that are both stiffer and more stable under plastic deformations. This work is part of a larger initiative (steeli.org) that aims to better understand and optimize the role of diaphragms in the seismic response of steel buildings.

1. Introduction

An effective seismic design of buildings includes the design of both a vertical lateral force resisting system (LFRS) and a horizontal LFRS, i.e., a diaphragm. The design requirements of the diaphragm are shifting, e.g., prior to ASCE 7-16 [1], the diaphragm was designed to remain elastic for design earthquakes (DE) [2] [3]. However, ASCE 7-16 implemented a new alternative diaphragm design method, where the diaphragm is designed for inelastic behavior [1]. And the new NEHRP design recommendations [4] include the design of diaphragms in rigid wall flexible diaphragm (RWFD) buildings, which specifically dictates a diaphragm with ductile behavior [5].

As buildings take on new shapes and intricate floor plans, diaphragms with complex shapes, that include cutouts and openings, become necessary. Therefore, rethinking and innovating new systems is a necessary response to the demand for efficient, sustainable, and resilient building designs. In Fischer, et al. [6], diaphragms in various building layouts are designed for maximum stiffness with the use of topology optimizations [7]. Topology optimization is a valuable tool for creating novel designs. However, optimized design may often be elaborate and complex, more than is practical possible in construction. As such, the optimized diaphragm designs were subjected to an interpretation resulting in a design that is viable for construction in Fischer, et al. [6].

In this paper, various diaphragm designs are subjected to a non-linear pushover analysis, to analyze and compare their inelastic response and ability to absorb energy. The plasticization is assumed to only affect the shear resistance of the deck, and a non-linear model affecting the shear strength and stiffness is developed and implemented for this analysis.

2. Setup and nonlinear model

Three diaphragm layouts and their designs from [6] are illustrated in Figure 1 with dimensions listed in Table 1. The rectangular diaphragm layouts are inspired by the SDII archetype building models [8], called *SDII* and *SDIICUT* in this paper, and DC Water headquarter building in Washington D.C. [9] inspired the DC-WASA configuration. Two diaphragm designs for each layout are developed by Fischer, et al. [6]: (1) a traditional designed diaphragm with deck orientation equal to zero, see Figure 1b, and (2) an interpreted optimized design, where both deck type and deck orientations are optimized, see Figure 1c and d. The scale of grey in Figure 1b and c is an indication of the

[1] Postdoctoral Fellow, Johns Hopkins University, winther@jhu.edu
[2] Postdoctoral Fellow, Danmarks Tekniske Universitet, feferr@dtu.dk
[3] Associate Professor, Johns Hopkins University, jkguest@jhu.edu
[4] Professor, Johns Hopkins University, schafer@jhu.edu

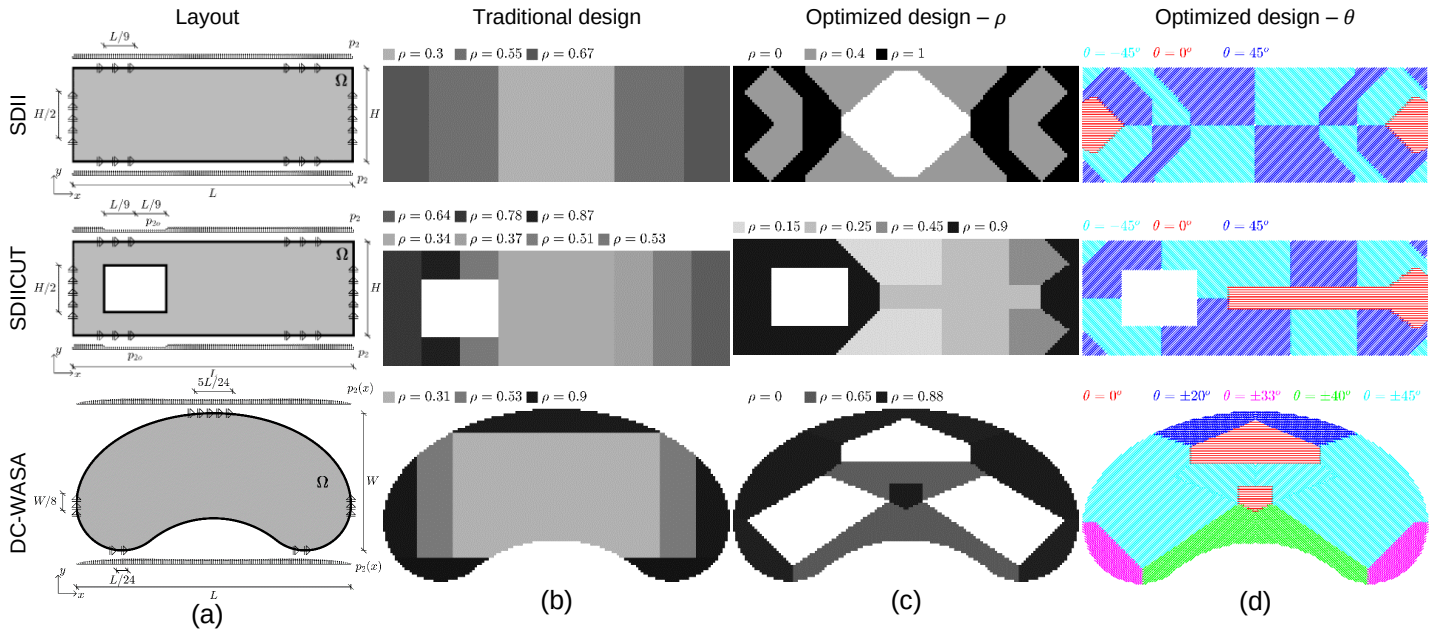

Figure 1: Diaphragm layouts and designs. (a) Geometry, loadings and boundary conditions of the diapharagm examples considered. (b) traditional diaphragm design with $\theta = 0$. (c-d) compliance optimized and post-processed layouts (c) deck type (d) deck orientation. The grayscale reflects the distribution of the selector ρ, thus the variation of stiffness and strength (mean(ρ) ≈ 0.5 is maintained for all the designs). Colored lines indicate different orientations (θ) of the strong material axis.

stiffness of the deck type at that location, with white being a deck with little stiffness and strength and black being the stiffest deck available. The lines in Figure 1d indicate the different orientations (θ) of the strong axis of the decks.

Table 1: Geometrical dimensions and data for the diaphragms examples

Property	US units	SI units
L – length	300 ft	91.44 m
H – height	100 ft	30.48 m
W – width	150 ft	45.72 m
F_{px} (SDII)	262 kips	1165 kN
F_{px} (SDIICUT)	245 kips	1090 kN
F_{px} (DC-WASA)	285 kips	1266 kN

2.1 Material model

Steel deck diaphragms are connected with fasteners to the underlying structure (structural fasteners) and along the sides to other decks (sidelap fasteners). The diaphragm is designed for its shear strength and stiffness according to AISI S310 [10]. The diaphragm strength and stiffness are a function of the strength/stiffness of the fasteners and the number of fasteners. Torabian, et al. [11] tested different steel deck fasteners and observed shear tearing and bearing of the deck at the fastener or fracture of the deck around a weld. The sidelap connections are generally the weaker of the two, and when the sidelap connection begins to tear or fracture it will impact the shear stiffness of the deck, as the shear transfer mechanism is weakened. The diaphragm is considered functional if the structural fasteners are still effective, i.e., the deck is still attached to the underlying structure. Testing has shown that at a shear angle of approximately 4%, the structural connections begin to separate from the deck, where the deck fails.

According to this reasoning, the non-linear model assumes that plasticization of the deck is solely driven by shear deformations and by reducing the shear stiffness after initial yield, i.e., initiating tearing at the sidelap fasteners. The optimized diaphragm designs have different deck orientations, therefore is the plastic formulation written in the local material coordinate system. Furthermore, the shear stress-strain work conjugate pair (τ_0, γ_0) in the plastic formulation is decoupled from the other stress/strain terms in the local material coordinate system, which is a 1D plasticity problem [12] on the shear stress/strain. The yielding function is as follows:

$$\psi = |\tau_0| - \tau_Y \tag{1}$$

where τ_0 is the shear stress in the local material coordinates, and $\tau_Y(\rho_e)$ is the yielding shear stress, based on the deck's shear strength $V(\rho_e)$:

$$\tau_Y = 0.8\, V(\rho_e) \tag{2}$$

The material model assumes an elasto-plastic response with a bilinear curve, that is defined by the yielding stress, $\tau_y(\rho_e)$, the ultimate and yielding shear angles:

$$\gamma_u = 4\% \tag{3}$$

$$\gamma_y = \frac{\tau_Y}{G'} \tag{4}$$

where G' is the initial shear stiffness of the deck and G'_t is the tangent stiffness after yielding:

$$G_t'(\rho_e) = \frac{0.2\,V(\rho_e)}{\gamma_u - \gamma_Y(\rho_e)} \quad (5)$$

The stiffness and strength (G', V, E_1' and E_2') of the deck are assumed a linear function of the variable ρ, with $(\cdot)$ being the stiffness or strength:

$$(\cdot)(\varrho) = \left(\rho\left(1 - \frac{\varrho_{min}}{\varrho_{max}}\right) + \frac{\varrho_{min}}{\varrho_{max}}\right)(\cdot)_{max} \quad (6)$$

where $G'_{max}, V_{max}, E'_{1,max}$ and $E'_{2,max}$ and the ratio $\varrho_{min}/\varrho_{max}$ are listed in Table 2.

Table 2: Equivalent moduli and shear strength of bare steel decks.

Property	US units	SI units
$E_{1_{max}}'$	2885 kips/in	505,200 kN/m
$E_{2_{max}}'$	0.8947 kips/in	156.7kN/m
G'_{max}	241.1 kips/in	942.1 kN/m
V_{max}	4995 lb/ft	3389 N/m
$\varrho_{min}/\varrho_{max}$	0.0525	

2.1 Non-linear model

The diaphragm designs are subjected to a "pushover analysis" (the model only consists of the diaphragm and as such, a pushover analysis of the entire building structure is not considered but just the behavior of the diaphragm), where the non-linear equilibrium equation in Eq. 7 is solved with Newton-Raphson method:

$$\boldsymbol{r}(u_k) = \boldsymbol{F}_{int}(u_k) - \boldsymbol{F}_{ext,k} = \boldsymbol{0} \quad (7)$$

where $\boldsymbol{F}_{int}$ is the internal force, $\boldsymbol{F}_{ext,k}$ is the external force at increment k and $\boldsymbol{r}(u_k)$ is the residual difference. The external load is applied over 200 steps: $\boldsymbol{F}_{ext,k} = \lambda_k \boldsymbol{F}_{px}$, with load multipliers $\boldsymbol{\lambda} = \{0, \lambda_1, \lambda_2, \ldots, 1\}$ and $\boldsymbol{F}_{px}$ is the total design load of the diaphragm, see Table 1.

The analysis is stopped when either the total design load is reached, or the diaphragm fails at a shear angle of $\gamma_u = 4\%$, at which the structural fasteners detach from the underlying structure.

3. Pushover results and discussion

The six diaphragm designs (three traditional and three optimized) were subjected to a pushover analysis. The areas of plasticization are illustrated in Figure 2 at the time of failure and Figure 3 shows the internal work, the plastic portion of the work, and the shear strains as a function of the load multiplier, λ. The plastic potion of the work is associated with the energy dissipation of the decks. The internal work ($\mathcal{W}$) and plastic portion of the work ($\mathcal{W}_p$) are determined at each iteration as follow:

$$\mathcal{W}_k = \int_\Omega \boldsymbol{\sigma}^t\, \boldsymbol{\varepsilon}\, d\Omega \quad (8)$$

$$\mathcal{W}_{p,k} = \int_\Omega \gamma_p\, \tau_Y\, d\Omega \quad (9)$$

Where the total work $\mathcal{W}$ and total plastic work $\mathcal{W}_p$ is the sum of work at each previous iteration.

From Figure 2 one can observe:

- First yield (blue circles) occurs for all diaphragm examples at the boundary conditions.
- All traditional designs have localized areas of plasticization near the boundary conditions with no plastic zones in the interior of the diaphragm.
- The optimized designs have more areas of plasticization which are located at the boundary conditions and along the lines of high stiffness contrast. Observe that the lines of plasticization are corresponding to the transition of dark to light areas in Figure 1c.

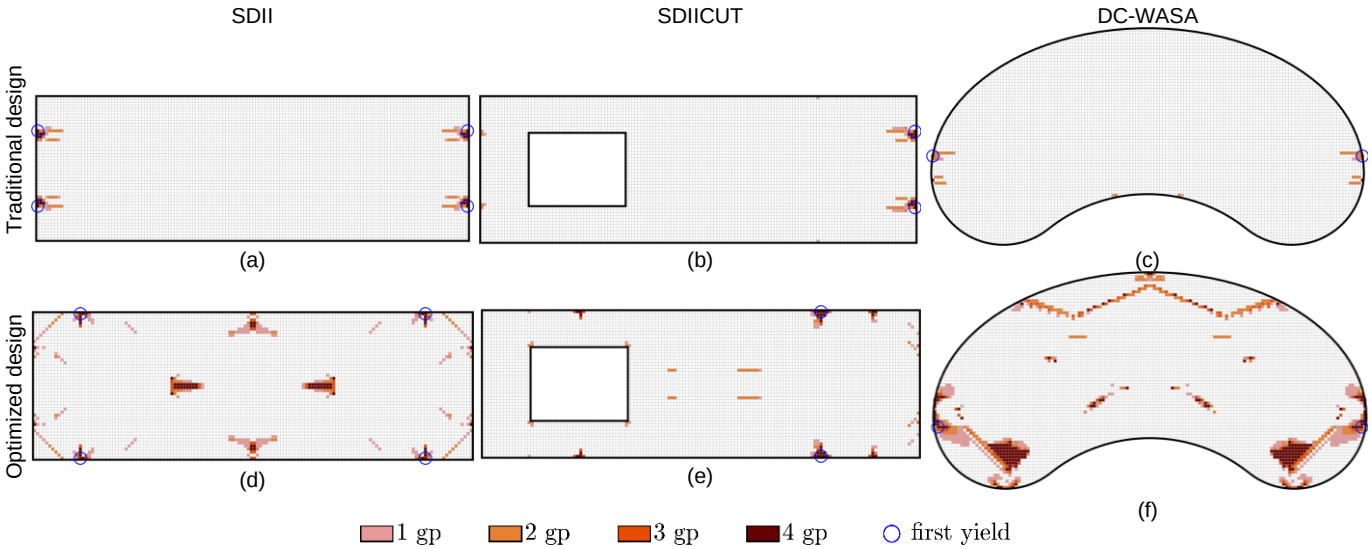

Figure 2: Plasticized regions at the failure stage for the traditional (left column) and optimized (right column) designs. The color distribution is according to the number of Gauss points within an element that are yielding and the circles indicates the location of initial yielding.

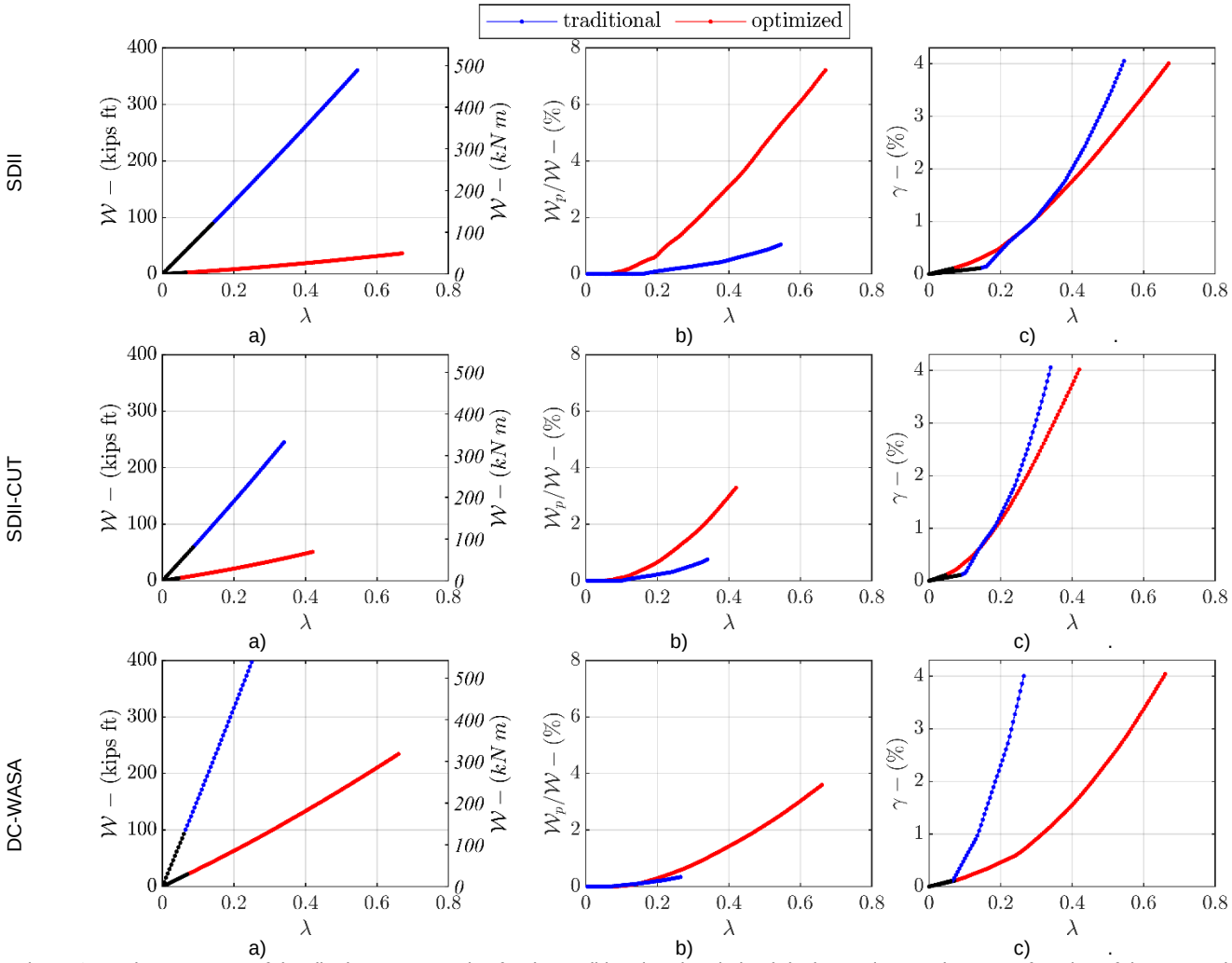

Figure 3: Pushover curves of the diaphragm examples for the traditional and optimized designs. Figures show as a function of the external load multiplier the evolution of a) the total cumulative work, b) the plastic work fraction of the total work, and c) the maximum shear angle.

- From these figures, one can get that the optimized designs have a better ability to redistribute stresses.

The response curves in Figure 3 can add to the above remarks with the following observations:

- The optimized designs are much stiffer than the traditional designs, as the cumulative internal work, $\mathcal{W}$, is lower for the optimized designs in both the elastic and plastic ranges of the response, see Figure 3a. This is somewhat expected, as the diaphragms are optimized for minimum compliance in the elastic range, but they were not optimized to consider the plastic response.
- The optimized designs have a better capability to dissipate energy compared to the traditional designs, as the ratio $\mathcal{W}_p/\mathcal{W}$ is higher than the traditional designs for all three layouts and throughout the analysis, see Figure 3b.
- The three traditional designs dissipate less than 1% of the total work in the pushover analysis, whereas the 3 optimized designs dissipate 3-7% of the total work.
- Figure 3c indicates that the traditional designs experience a sudden increase in total shear angle when yielding begins, compared to the gradual increase in total shear angle for the optimized designs.

The elastic portion of the response are specified with black dots in the curves in Figure 3. This allows for the comparison of onset of initial yield, which occurs earlier for the optimized designs, expect for the DC-WASA diaphragm. This is expected, as the highest elastic stresses are observed at the boundary conditions for all designs, and the traditional designs are designed with high strength deck types at the ends that can delay the start of first yield. However, because of its ability to redistribute stresses across the diaphragm the optimized designs can reach a higher capacity at the time of failure compared to the traditional designs, this applies to all three diaphragm layouts.

In general, the optimized designs are performing better than the traditional designs, demonstrating that even linear elastic topology optimization can potentially provide better results. The stark difference in shear angle response for the DC-WASA diaphragm in Figure 3c, indicates the potential of

topology optimization in designing complicated layouts and demands.

The concept of controlling the location of plasticization in the diaphragm is not new, Koliou, et al. [5] have proposed a diaphragm design method with distributed yielding, where the interior of the diaphragm is dissipating energy under seismic loading. This is found to be a superior design compared to traditional diaphragm design where plasticization is concentrated near the edges. This design method is in line with the observations made in this paper.

The analyzed diaphragms in this paper did not include any considerations for the underlying structure such as chord and collectors that are a main component in the design of diaphragms, but solely the response and behavior of the diaphragm deck alone. By including the underlying structure in the analysis, indicate that the diaphragm has improved behavior, which includes a delayed onset of first yield and larger zones of plasticization which will increase the dissipated energy in the diaphragm, in that the underlying structure can distribute concentrated forces near the boundary conditions to a larger area of the diaphragm [13].

4. **Conclusions**

Topology optimized and traditional designed diaphragms were investigated and compared for their ability to undergo plastic deformations in a pushover analysis. According to the results presented, even though the optimized decks were designed to maximize the linear elastic stiffness, they also performed well in the non-linear range, especially when compared to the traditional diaphragm designs. The optimized designs were found to have a higher load carrying capacity at the time of failure, they had a stiffer behavior, both in the elastic and plastic range, and they had a better ability to redistribute stresses, resulting in a distributed damage pattern, and a higher amount of dissipated energy.

The results demonstrate that topology optimization can be applied to designing novel diaphragm configurations, even when complicated responses and practical effects are considered, such as non-linearity. However, the onset of first yield occurs earlier for the optimized designs, which may hinder the deck's serviceability under operational loads. In addition, it is somewhat more difficult to anticipate the exact location(s) of initial yield and the stress redistribution pattern for the optimized designs as opposed to the traditional ones. These issues will be addressed in future work, such as, including stress constraints into the optimization formulation to postpone the onset of initial yield, or by explicitly accounting for damage in the formulation, ensuring that diaphragms can be designed to have maximum stiffness and damage absorption properties.

5. Acknowledgments

The authors gratefully acknowledge the financial support funded by the American Iron and Steel Institute, the American Institute of Steel Construction, the Steel Deck Institute, the Metal Building Manufacturers Association, the Steel Joist Institute and the US National Science Foundation through grant CMMI-1562821. And support from the National Aeronautics and Space Administration (NASA) under Grant No. 80NSSC18K0428. Also, the ideas and contributions from collaborators in the Steel Diaphragm Innovation Initiative (SDII) effort are acknowledged. Any opinions, findings, and conclusions or recommendations expressed in this material are those of the author(s) and do not necessarily reflect the views of the National Science Foundation or other sponsors.

References

[1] ASCE 7-16, "Minimum Design Loads and Associated Criteria for Buildings and Other Structures," American Society of Civil Engineers, Reston, Virginia, 2016.

[2] R. Sabelli, T. A. Sabol and W. S. Easterling, "Seismic Design of Composite Steel Deck and Concrete-filled Diaphragms, A Guide for Practicing Engineers," National Institute of Standards and Technology (NIST), Gaithersburg, MD, 2011.

[3] R. Park, T. Paulay and D. K. Bull, "Seismic Design of Reinforced Concrete Structures," New Zealand Concrete Society, Technical Report No. 20, 1997.

[4] FEMA, "NEHRP Recommended Seismic Provisions for New Buildings," prepared by the, Washingtonn, D.C., 2020.

[5] M. Koliou, A. Filiatrult, D. J. Kelly and J. Lawson, "Buildings with rigid walls and flexible roof diaphragms. II: Evaluation of a new seismic design approach based on distributed diaphragm yielding," *Journal of Structural Engineering,* vol. 142, no. 3, 2016b.

[6] A. Fischer, J. Guest and B. Schafer, "Topology optimization of steel deck building diaphragms," *Journal of Constructional Steel Research,* vol. 191, 2022.

[7] M. P. Bendsøe and O. Sigmund, Topology Optimization: Theory, Methods and Applications, Springer, 2004.

[8] S. Torabian, M. Eatherton, W. Easterling, J. Hajjar and B. Schafer, "SDII Building Archetype Design v1.0," CFSRC Report R-2017-04, permanent link: jhir.library.jhu.edu/handle/1774.2/4063, 2017.

[9] J. Grant and S. Stewart, "Going with the Flow," *AISC Modern Steel Construction,* pp. 28-34, March 2018.

[10] AISI, "North American Standard for the Design of Profiled Steel Diaphragm Panels," S310, American Iron and Steel Institute, 2013.

[11] S. Torabian, D. Fratamico, K. Shannahan and B. Schafer, "Cyclic Performance and Behavior Characterization of Steel Deck Sidelap and Framing Connections," *2018 International Specialty Conference on Cold-Formed Steel Structure,* 2018.

[12] R. I. Borja, Plasticity: Modeling and Computation, Springer Verlag, 2013.

[13] A. W. Fischer, "Seismic Performance and Topology Optimization of Building Diaphragms," Johns Hopkins University, Baltimore,MD, 2021.